ACS SyntheticBiology

pubs.acs.org/synthbio

Research Article

Development of a Transcription Factor-Based Diamine Biosensor in *Corynebacterium glutamicum*

Nannan Zhao, Jie Song, Hao Zhang, Ying Lin, Shuangyan Han, Yuanyuan Huang,* and Suiping Zheng*

Cite This: *ACS Synth. Biol.* 2021, 10, 3074−3083

Read Online

ACCESS | Metrics & More | Article Recommendations | Supporting Information

ABSTRACT: Diamines serve as major platform chemicals that can be employed to a variety of industrial scenarios, particularly as monomers for polymer synthesis. High-throughput sensors for diamine biosynthesis can greatly improve the biological production of diamines. Here, we identified and characterized a transcription factor-driven biosensor for putrescine and cadaverine in *Corynebacterium glutamicum*. The transcriptional TetR-family regulatory protein CgmR (CGL2612) is used for the specific detection of diamine compounds. This study also improved the dynamic range and the sensitivity to putrescine by systematically optimizing genetic components of pSenPut. By a single cell-based screening strategy for a library of CgmR with random mutations, this study obtained the most sensitive variant $CgmR_{I152T}$, which possessed an experimentally determined limit of detection (LoD) of ≤0.2 mM, a K of 11.4 mM, and a utility of 720. Using this highly sensitive putrescine biosensor $pSenPut_{I152T}$, we demonstrated that $CgmRI_{152T}$ can be used as a sensor to detect putrescine produced biologically in a *C. glutamicum* system. This high sensitivity and the range of CgmR will be an influential tool for rewiring metabolic circuits and facilitating the directed evolution of recombinant strains toward the biological synthesis of diamine compounds.

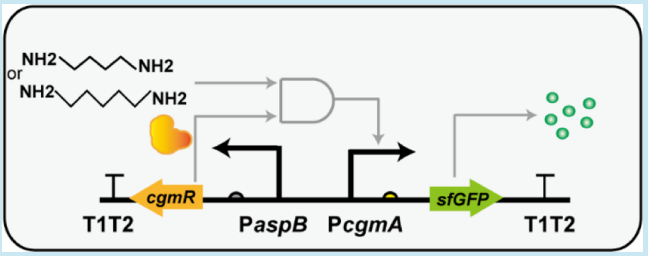

KEYWORDS: *Corynebacterium glutamicum, diamines, transcription factor, biosensor, biological synthesis*

INTRODUCTION

Engineering microbial cell factories to produce valuable chemicals and fuels is currently an attractive alternative to chemical synthesis. Nevertheless, existing studies primarily concentrate on building pathways for producing various compounds.[1−3] The discovery and engineering of novel pathways and enzyme variants are frequently restricted due to the shortage of fast and efficient evaluation methods or screening tools. Genetically encoded biosensors prepared with fluorescence-based genetic circuit devices offer influential high-throughput screening tools (HTSs) to acquire high-performing strains from genetically diverse strain libraries.[4,5] Thus, transcriptional biosensors have emerged as valuable tools for metabolic engineering. Meanwhile, they significantly accelerate design−build−test cycles.

Transcription factor-based biosensors (TFBs) are composed of three parts: transcription regulators (TRs), response elements, and reporter elements. The reporter element is usually a fluorescent protein whose expression is controlled by ligand-induced transcriptional regulators. Therefore, transcriptional regulators can be engineered to monitor intracellular target molecules. At present, transcription factor-based biosensors are frequently used for high-throughput screening,[4,6,7] adaptive evolution,[8,9] real-time monitoring,[5] and single-cell analysis.[10] In addition, TF-based biosensors can be engineered as regulatory switches to dynamically regulate metabolic fluxes and decrease toxic intermediate accumulation.[11] However, biosensors with natural evolution cannot supervise numerous target metabolites. Progress of synthetic biology has stimulated the advancement in various genetic devices and biological modules that have greatly facilitated the development of biosensors.[12] Response dynamics are an important feature of genetically encoded biosensors.[13] To increase the dynamic response of the biosensor system (i.e., the induced expression level in comparison with the uninduced expression level), the usual strategy is to construct a hybrid promoter with stronger affinity by changing the sequence, position, and number of operons bound by transcription factors.[14−16] Another strategy that can be used to modulate the response of the biosensor is to alter the TR expression level by using promoters or ribosome binding site (RBS) sequences at different strengths.[15,17,18] In recent years, lots of studies involving TF-based sensors in HTSs have attempted to alter the ligand-binding properties of several TRs by protein engineering.[18−20] For instance, the well-known transcriptional

Received: August 1, 2021
Published: October 18, 2021

https://doi.org/10.1021/acssynbio.1c00363
ACS Synth. Biol. 2021, 10, 3074−3083

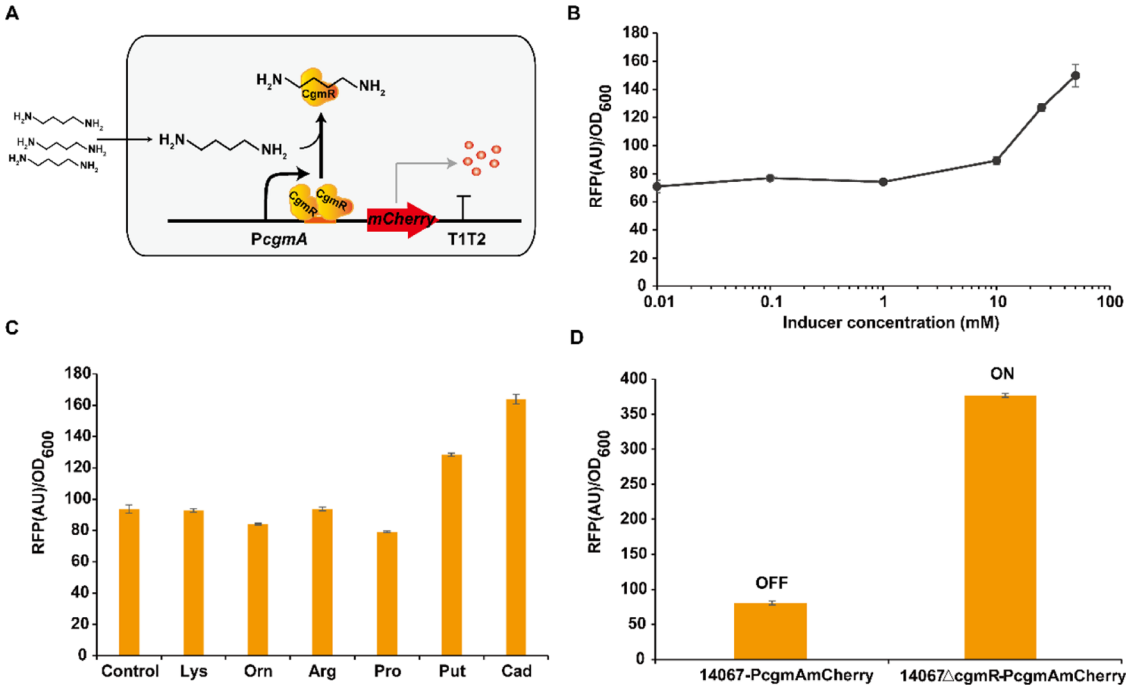

Figure 1. Development of the CgmR-based putrescine biosensor pSenPut. (A) Diagram of *C. glutamicum* ATCC 14067 harboring the chromosome-encoded CgmR and the biosensor plasmid PcgmAmCherry to test CgmR putrescine sensing. The cell-based biosensor works by the input (diamine) entering the cell being detected by the sensor component CgmR, which then counteracts its ability to bind to P*cgmA* and thus causes the generation of the red reporter protein (output). (B) Fluorescence data of CgmR-based biosensors for putrescine from 0 to 100 mM. (C) Various amino acids or diamine compounds were detected at a concentration of 20 mM by pSenPut. L-lysine (Lys), L-ornithine (Orn), L-arginine (Arg), 1,3-propylenediamine (Pro), 1,4-butanediamine (Put), and 1,5-pentanediamine (Cad). The fluorescence displayed at a background level without any treatment was used as the control. (D) Strength of P*cgmA* at the "OFF" and fully "ON" states (Supporting Information Figure S1). Besides, the cell culture fluorescence was normalized by cell density. Data are shown as the mean and standard deviation of independent triplicates.

activator AraC of *Escherichia coli*, which was originally used to detect L-arabinose, evolved to sense new effector molecules, such as arabinose,[21] mevalonate,[22] and triacetic acid lactone.[23] In contrast, some natural TRs, such as LysG of *Corynebacterium glutamicum* ATCC 13032, have relaxed ligand specificity, which also limits their efficient utilization in a biosensor system. The biosensor pSenLys, which is composed of LysG and its targeting promoter that controls LysE expression, appears to be a useful instrument for the identification of *C. glutamicum* L-lysine synthesis strains but cannot be used for screening L-histidine and L-arginine synthesis strains.[4] The semirational engineering design of LysG shows that it does not bind to L-lysine but maintains binding ability to L-histidine and L-arginine. The rationally designed LysG variant LysG-A219L with a narrow ligand spectrum was then used to construct the biosensor pSenHis, which can identify the L-histidine-producing *C. glutamicum* variants by fluorescence-activated cell sorting (FACS) analysis.[19]

Diamine compounds, such as 1,4-diaminobutane (putrescine) and 1,5-diaminopentane (cadaverine), have attracted considerable attention because they can be used as monomers of synthetic polyamide plastics in the industry. In addition, they can be used in the synthesis of pesticides, metal ion chelators, surfactants, and oil and fuel additives. With increasing attention to natural resources and environmental issues, a greater number of studies have focused on utilizing renewable feedstocks by microbial cell factories for the synthesis of diamines. To date, *E. coli* and *C. glutamicum* are still the preferred host strains for metabolic engineering to synthesize diamine compounds.[24−27] Compared with *E. coli*, *C. glutamicum* lacks natural putrescine and cadaverine synthetic pathways and therefore requires the introduction of heterologous ornithine decarboxylase or lysine decarboxylase. However, *C. glutamicum* has its own advantages in the synthesis of putrescine and cadaverine, such as a strong metabolic flux toward lysine and glutamate, high tolerance, and no degradation pathways.[28] Many excellent review articles have focused on research, investigating the production of putrescine and cadaverine using metabolic engineering strategies.[1,29] Due to the lack of high-throughput methods to assess the quality of genetic variation or production conditions, biobased diamines are short of competitiveness against diamines made by chemical synthesis. Recently, the putrescine-responsive biosensor transcription factor PuuR was designed successfully in *E. coli*, and the whole-cell biosensor proved specific only for putrescine over 1,3-diaminopropane, cadaverine, and 1,6-diaminohexane. However, the low dynamic range may limit its application in biosensor systems.[14]

The *cgmAR* operon, which is able to encode one putative permease and one transcriptional TetR-family repressor CgmR, had been already proved to bind −37 to −6 bp upstream of *cgmA*, which is called *cgmO*.[30] Electrophoretic mobility shift assay (EMSA) demonstrated that putrescine and other diamines perturbed CgmR-*cgmO* complex formation but not free *cgmO* DNA migration.[24,30] The above results demonstrate that CgmR is probably a putrescine-sensitive transcription factor, which is able to take control of putative permease CgmA expression. Thus, CgmR has the potential to be used as a biosensor of putrescine. In this study, we demonstrated that the TetR-family regulator CgmR is indeed a

https://doi.org/10.1021/acssynbio.1c00363
ACS Synth. Biol. 2021, 10, 3074−3083

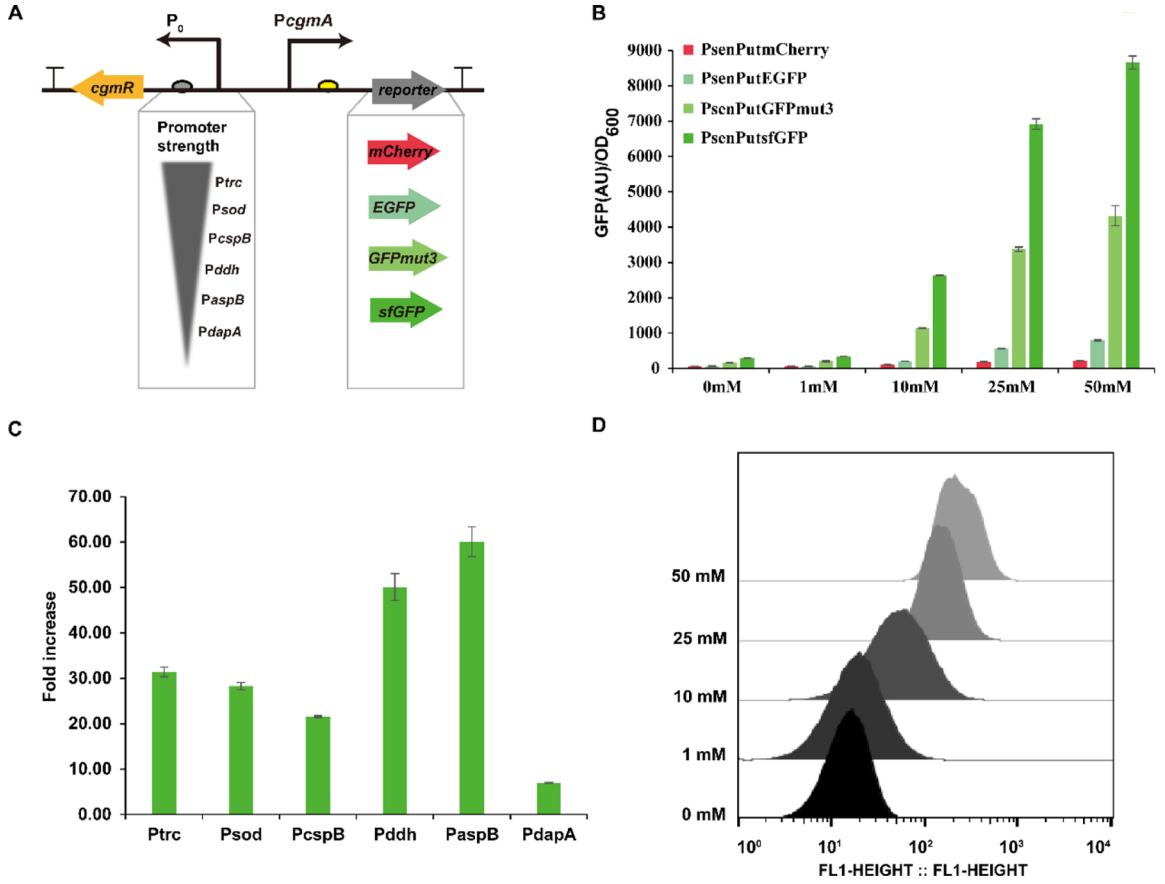

Figure 2. Optimization and quantitative analysis of pSenPut and pSenPut variant responses. (A) Schematic representation of the strategy for developing pSenPut. (B) Effect of reporter protein replacement in pSenPut. (C) Optimization of CgmR expression in pSenPut, with the relative strength of the promoter driving *cgmR* on the left. Cg14067Δ*cgmR* was transformed by electroporation with these constructs. Fluorescence data of different expression levels of CgmR-based biosensors for putrescine from 0 to 100 mM were fitted to the Hill equation to derive biosensor performance characteristics and the utility for the six different promoters calculated from the Hill functions. Values indicate the means ± SDs of three independent experiments. (D) Correlations between the concentration of exogenous putrescine and specific fluorescence measured 24 h after the addition of putrescine at the indicated concentrations to Cg14067Δ*cgmR* cells harboring pSenPut. Representative histograms from three independent rounds of FACS are denoted.

diamine biosensor. For improving both the signal-to-noise ratio and sensing sensitivity, we systematically optimized the genetic components of pSenPut. Our strategy included (a) optimization of a reporter gene, (b) optimization of a promoter for controlling a regulator, and (c) engineering of transcriptional regulator CgmR through FACS. For demonstrating sensor utility, we showed that the use of $CgmR_{I152T}$ as a sensor can investigate intracellular putrescine concentrations and detect extracellular putrescine produced biologically in a *C. glutamicum* system.

RESULTS AND DISCUSSION

Identification and Development of CgmR as a Diamine Biosensor. As a promising transcription factor for sensing putrescine CgmR and its cognate *cgmA* promoter P*cgmA*, which naturally exist in *C. glutamicum*, CgmR-based biosensors in *C. glutamicum* were designed and constructed. The cognate promoter positioned upstream of the reporter gene could play the role of a CgmR-repressive genetic element to express the reporter protein in a manner that depends on the intracellular concentration of putrescine.

To screen the ability of CgmR to sense putrescine, the 140-bp upstream of *cgmA* was cloned upstream of *mCherry* on the pEC-T18-mob2 (2−4 copies/genome) plasmid and transferred into *C. glutamicum* ATCC 14067. Without intracellular and environmental putrescine, CgmR can be integrated with the operator sequence (*cgmO*) and represses *mCherry* transcription. The presence of putrescine causes binding of CgmR derived from the *C. glutamicum* ATCC 14067 chromosome, which causes derepression of the P*cgmA* promoter, resulting in *mCherry* gene expression and fluorescence emission (Figure 1A). We first studied the response of CgmR-based putrescine biosensors to 0−100 mM extracellular putrescine concentrations. As shown in Figure 1B, the expression of the fluorescent protein began to increase, when the putrescine concentration was 10 mM, and increased with the increase of putrescine concentration, reaching the maximum at 50 mM, suggesting that the repressor protein CgmR and the corresponding response *cgmA* promoter can be used as a potential putrescine sensor. For examining ligand specificity of pSenPut, it was adopted for L-lysine (Lys), L-ornithine (Orn), L-arginine (Arg), 1,3-propylenediamine (Pro), 1,4-butanediamine (Put), and 1,5-pentanediamine (Cad). pSenPut sensed 1,4-butanediamine and 1,5-pentanediamine, whereas 1,3-propylenediamine and intermediates, such as L-lysine, L-ornithine, and L-arginine in the diamine biosynthesis pathway, were unable to promote *mCherry*

https://doi.org/10.1021/acssynbio.1c00363
ACS Synth. Biol. 2021, 10, 3074−3083

expression above the background level even at high concentrations (20 mM) (Figure 1C).

The promoter activity was assessed under two genetic backgrounds, one was the wild-type *C. glutamicum* ATCC 14067 (Cg14067) and another was Δ*cgmR*. Cg14067 harbors the intact *cgmR* gene but lacks natural putrescine synthetic pathways, revealing *cgmA* promoter's basal activity under the repressed status, namely, the "OFF" status, whereas the Δ*cgmR* strain was defective in the chromosomal *cgmR* gene and able to imitate the *cgmA* promoter's completely derepressed status, which is the "ON" state (Supporting Information Figure S1). Strains Cg14067 and Δ*cgmR* harboring the plasmid PcgmAmCherry were afterward grown in the BHI medium at 30 °C, followed by measurement of cell culture fluorescence (normalized by cell density). Red fluorescence outputs of P*cgmA* from Δ*cgmR* were obviously higher than those of Cg14067 (Figure 1D), and the dynamic range (namely, induced expression level in comparison with uninduced expression level) was 4.7.

Optimization and Characterization of pSenPut. This study improved pSenPut's response characteristics through optimization, and it is based on optimizing a reporter gene and a promoter for controlling a regulator (Figure 2A). We first constructed four different pSenPuts in this study (Figure S2). The first was pSenPutmCherry, which contained the *cgmR* gene subject to the control of the constitutive p*trc* promoter along a direction against that of transcription of P*cgmA*−*mCherry* fusion. On this basis, we substituted the *mCherry* reporter gene with the *egfp*, *gfp*mut3, and superfolder GFP (*sfgfp*) genes to produce pSenPutEGFP, pSenPutGFPmut3, and pSenPutsfGFP, respectively. pSenPutsfGFP showed the highest fluorescence to all tested concentrations of putrescine (1−50 mM) compared with the other constructs, and the fold increases of pSenPutmCherry, pSenPutEGFP, pSenPutGFPmut3, and pSenPutsfGFP were 4.0, 12.0, 25.7, and 29.6, respectively (Figure 2B). The above findings showed that replacement of fluorescent proteins is a high-efficiency strategy to improve the sensor signal-to-noise ratio. To further optimize CgmR expression in pSenPutsfGFP, we substituted the promoter with various native promoters with different strengths of *C. glutamicum*[31] (Figure S2, Table S1). As seen in Figure 2C, we calculated every circuit's utility through calculating the relative input range and multiplying with the output fold induction.[32] The results showed that the circuit with the P*aspB* promoter showed the highest output fold induction (60.0×) and the second highest relative input range (5.5×), while pSenPutsfGFP-PaspB circuit's utility was measured as 330, exceeding the level of the pSenPutsfGFP-Ptrc circuit (193). Promoter optimization or engineering is one of the most commonly used strategies for regulating the dose−response characteristics of transcription factor-based biosensors. This regulation can both affect the binding ability of inducers and TFBs.[33] Strong promoters result in low leaky expression and low maximum expression. Sometimes, strong promoters cause a metabolic load in living cells, which simultaneously influences natural folding of TFs.[34] However, weak promoters do not produce large changes in expression during activation, resulting in high leakage expression. In conclusion, moderate-intensity promoter-controlled sensors can produce appropriate TFBs dose−response characteristics. It should be ascribed to the binding equilibrium between the polymerase and promoter.[12]

For quantitatively assessing pSenPutsfGFP-P*aspB* responses to putrescine, we calculated fluorescence at the single-cell level in Cg14067ΔcgmR cells harboring pSenPutsfGFP-PaspB in BHI medium at various putrescine concentrations (up to 50 mM). Fluorescence could be merely observed when putrescine existed (Figure 2D). The minimal concentration of putrescine required for the response of the biosensor was 10 mM. Additionally, a close positive correlation existed between the fluorescence intensity and putrescine concentration.

Characterization of the Biosensor Performance for Diamines. For quantifying pSenPutsfGFP-PaspB's sensing characteristics (Figure 3A), the concentrations of either

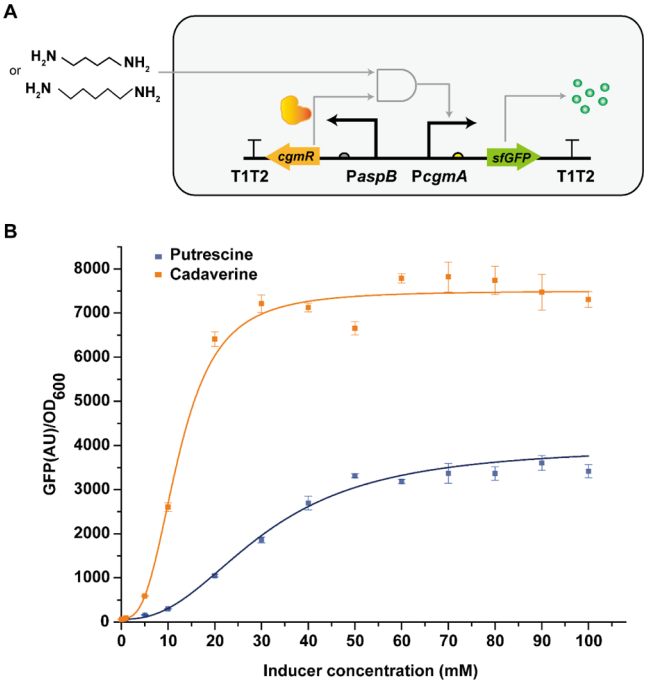

Figure 3. Characterization of biosensor performance for putrescine and cadaverine. (A) Schematic representation of pSenPut. Putrescine or cadaverine binds with CgmR derived from pSenPut, which then causes a derepression of the P*cgmA* promoter and the expression of the *sfgfp* gene. (B) Fluorescence data fit to the Hill equation to derive biosensor performance characteristics for putrescine and cadaverine. Values stand for means ± SDs of three independent experiments.

putrescine or cadaverine differed from 0.01 to 100 mM. The normalized fluorescence data were fitted to the Hill equation for assessing biosensor performance (Figure 3B). The results showed that pSenPutsfGFP-PaspB was sensitive to both putrescine and cadaverine, especially cadaverine. According to the fitting results, when the ligand is putrescine, K is approximately 30.8 mM and the detection limit is approximately 3.2 mM, and when the ligand is cadaverine, K is approximately 12.3 mM and the detection limit is approximately 1.5 mM (Table 1).

Besides, we studied the response of CgmR to longer carbon chain diamines, such as 1,6-diaminohexane and heptanediamine. The results showed that longer carbon chain diamines are more sensitive to CgmR, which was consistent with EMSA results in Nguyen et al. 2015,[24] and the expression of the fluorescent protein began to increase when the putrescine concentration was 1 mM (Figure S3). Because natural 1,6-diaminohexane (C6) and heptanediamine (C7) biosynthetic

https://doi.org/10.1021/acssynbio.1c00363
ACS Synth. Biol. 2021, 10, 3074−3083

Table 1. Best-Fitting Biosensor Performance Parameters and Standard Deviations[a]

ligands	Hill coef.	*K* (mM)	max	induction	LoD (mM)
putrescine	2.4 (0.2)	30.8 (3.0)	3981 (288)	63 (6)	≤3.2
cadaverine	2.9 (0.3)	12.3 (0.9)	7503 (215)	89 (6)	≤1.5

[a]Hill coef: predicted Hill coefficient. K: ligand concentration achieved half predicted maximal GFP expression. Max (normalized GFP): estimated maximal GFP expression. Induction: percentage of maximal GFP expression to basal expression. LoD: limit of detection.

pathways have not been reported, we put the research focus on 1,3-propylenediamine (C3), 1,4-butanediamine (C4), and 1,5-pentanediamine (C5).

Engineering the CgmR Transcriptional Regulator. To further improve the sensitivity of pSenPutsfGFP-PaspB to putrescine, we engineered the CgmR transcriptional regulator. On this basis, we proposed the single cell-based screening strategy for the CgmR library containing random mutations (Figure 4A). The *cgmR* mutant library could be formed through error-prone PCR and cloned in pSenPutsfGFP-PaspB, leading to library pSenPuts-*cgmR*^{Mut}. Then, it could be applied in the transformation of *E. coli* Top10. Plasmids could be separated from around 0.6 × 10^4 colonies for transforming Cg14067Δ*cgmR*. The 1 × 10^5 transformants were gathered to perform an in-depth survey. We enriched positive variants using high fluorescence signals based on putrescine, while removing false positive variants showing fluorescence short of putrescine. Following the three-round screening, the greatest 0.1% phenotypes were chosen to be putative hits and related fluorescence signals could be determined by putrescine in liquid BHI medium (Figure S4A,B). In particular, some showed a significantly increased fluorescence signal compared with the control when exposed to putrescine at 10 mM. We then measured the putrescine concentration response curves of several variants whose mutation sites were situated at the ligand-binding domain of CgmR. The results showed that different variants had different dynamic response ranges and sensitivities, with the single mutant I152T showing the best response characteristics (Figure 4B). It had a limit of detection (LoD) of ≤0.2 mM and a *K* of 11.4 mM. Besides, the utility of the CgmR$_{I152T}$ circuit could be measured as 720, exceeding that of the wild-type CgmR circuit (303) (Table S3). Then, we engineered the variant pSenPut$_{I152T}$ to maximize the sensor sensitivity. pSenPut$_{I152T}$ showed a marked enhanced fluorescence for putrescine and cadaverine, but the background signal was higher than the wild-type CgmR circuit pSenPut (Figure 4C). We further conducted the gel shift assays to test the DNA binding affinity and specificity of the variant pSenPut$_{I152T}$. Gel shift assays were basically performed as described previously.[24] The results showed that under the same conditions, the affinity between the variant CgmR$_{I152T}$

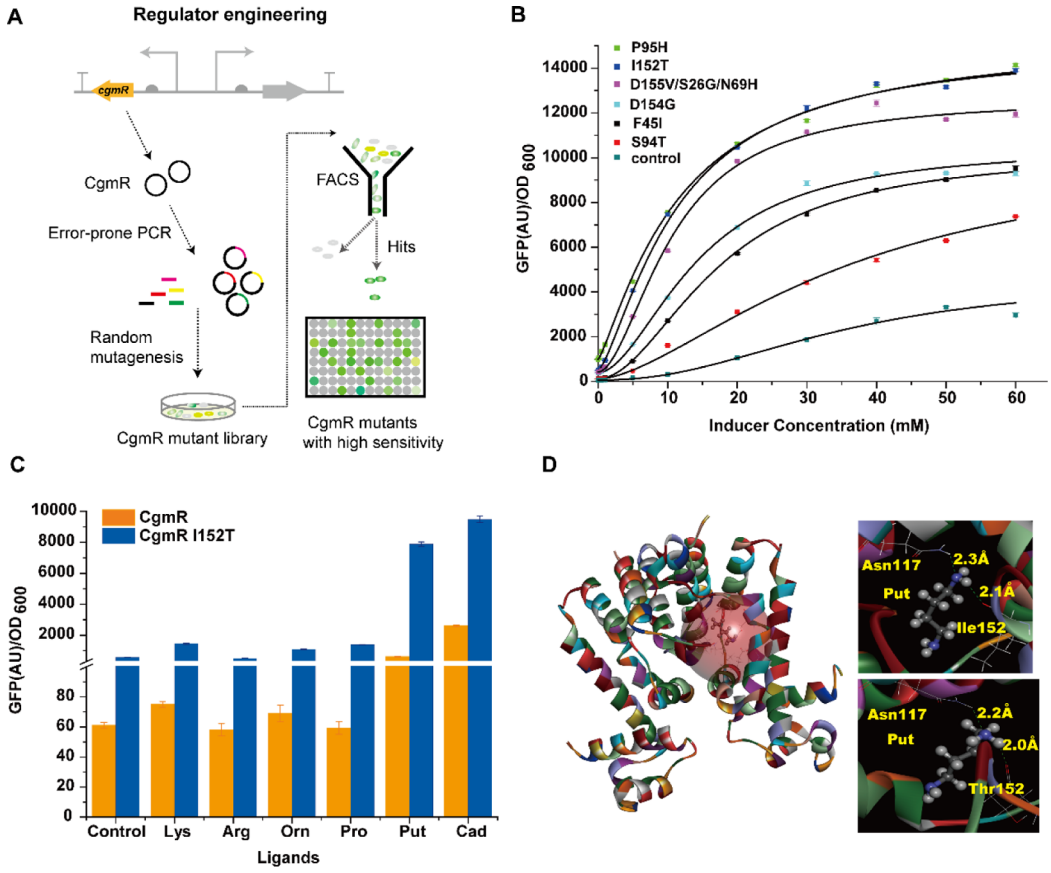

Figure 4. Engineering the CgmR transcriptional regulator. (A) Diagram of a single cell-based screening strategy for a library of CgmR with random mutations. (B) Quantitative analysis of the response of pSenPut and pSenPut variants to putrescine. (C). Ligand specificity of pSenPut and variant pSenPut$_{I152T}$. Amino acids or diamine compounds were detected at the concentration of 20 mM by pSenPut and pSenPut$_{I152T}$. L-lysine (Lys), L-arginine (Arg), L-ornithine (Orn), 1,3-propylenediamine (Pro), 1,4-butanediamine (Put), and 1,5-pentanediamine (Cad). (D) Homology modeling of pSenPut and pSenPut$_{I152T}$. Values denote the means ± SDs of three independent experiments.

https://doi.org/10.1021/acssynbio.1c00363
ACS Synth. Biol. 2021, 10, 3074−3083

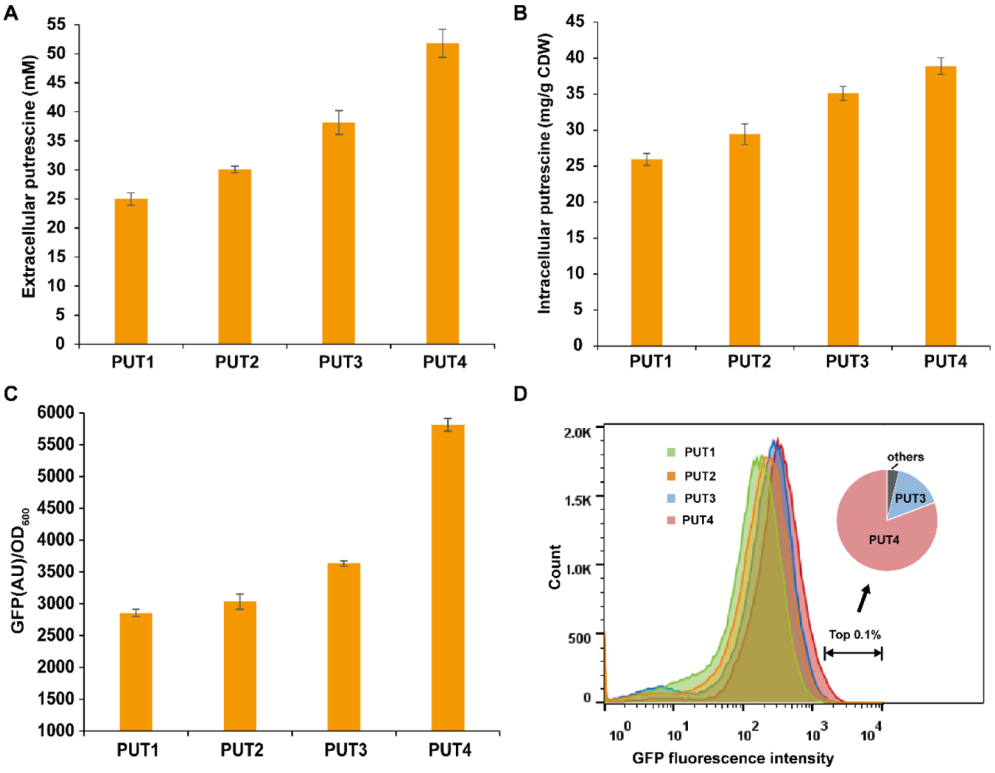

Figure 5. Detection of putrescine production in *C. glutamicum* via pSenPut$_{I152T}$. PUT1, PUT2, PUT3, and PUT4 derived from *C. glutamicum* ATCC 14067 by genetic modifications and equipped with the putrescine biosensor pSenPut$_{I152T}$. 0.5 mM IPTG was added to induce the overexpression of ornithine decarboxylases. (A) Putrescine production in liquid fermentation medium. (B) Intracellular putrescine concentration. Intracellular putrescine level was normalized by cell dry weight (CDW), which was assessed on the basis of an optical density of 1 corresponding to 0.25 g L^{-1} CDW at 600 nm wavelength. (C) Fluorescence intensities were measured and normalized by the cell intensities. (D) FACS results for the four strains mixed at equal OD. The putrescine strains were cultured in fermentation medium for 8 h to the late log phase. Strains exhibiting the top 0.1% of the fluorescence values were sorted. Subsequently, the screened strains were cultivated on agar plates at 30 °C for 36 h and distinguished by PCR or sequencing. Values stand for the means ± SDs of three independent experiments.

and DNA was weakened, which could explain the higher leakage of the sensor system PsenPut$_{I152T}$. However, the specificity of both is basically the same, and both of them show significant specificity only for putrescine and cadaverine and the longer chain diamines (Figure S5). For determining amino acid residues of CgmR, which are significant to the interaction with putrescine, we built in this study the homology model of CgmR under the crystal structure of *C. glutamicum* ATCC 13032 CgmR [Protein Data Bank (PBD) entry 2zoy]. As the nearest sequence, the sequence identity between them is 98.87%. Molecular docking results showed that residue I152 was expected to be located on one side of the inducer-binding site of CgmR; the hydrogen bond distance between CgmR and putrescine was changed from 2.1 to 2.0 Å by replacement of I152 in the CgmR regulator with threonine (T), while the hydrogen bond distance between N117 and putrescine was changed from 2.3 to 2.2 Å. The decreased hydrogen bond distance may be the main reason for the increased affinity of CgmR to putrescine (Figure 4D). Therefore, we used the I152T variant to evaluate the biosensor potential in high-throughput screening for putrescine-producing strains.

Detection of Putrescine Production in *C. glutamicum*. In order to verify the feasibility of this biosensor, this study explored the correlation of the responsive fluorescence signal with the intracellular putrescine concentration. The most sensitive pSenPut$_{I152T}$ plasmid was transformed into a series of *C. glutamicum* strains harboring ornithine decarboxylase on IPTG-inducible orthogonal plasmids (Table S1). These putrescine overproduction strains were cultivated for 72 h. The bacterial cells were harvested, and the intracellular and the extracellular levels of putrescine were quantified by HPLC. The putrescine production abilities of the four strains were in the order of PUT1 < PUT2 < PUT3 < PUT4 (Figure 5A). The intracellular putrescine concentrations were on the same order suggesting that higher-level putrescine producers tend to accumulate more putrescine in vivo (Figure 5B). The fluorescence intensity related to these strains was subsequently contrasted. The four strains showed fluorescence intensities in the order of PUT1 < PUT2 < PUT3 < PUT4 (Figure 5C), which was consistent with the order of putrescine production capabilities. Generally, the above findings proved that the putrescine biosensor reported putrescine production titers during shake flask fermentation. In order to verify whether the biosensor can effectively distinguish different putrescine producers and classify hyperproducing strains efficiently, we further evaluated the sorting property of the pSenPut$_{I152T}$ sensor plasmid. The GFP fluorescence intensities of the four strains could be measured using flow cytometry at 8 h of fermentation. Based on the obtained findings, there existed a significant growth of specific GFP fluorescence from PUT1 to PUT4. Afterward, we classified all colonies with the highest 0.1% fluorescence values and verified these screened colonies through PCR and sequencing analysis. According to Figure 5D, 80.77% screened cells had been demonstrated to have PUT4 strains, indicating that high-yield putrescine strains can

https://doi.org/10.1021/acssynbio.1c00363
ACS Synth. Biol. 2021, 10, 3074−3083

be selected with high efficiency based on the developed biosensor.

CONCLUSIONS

In this study, we first identified and characterized a transcription factor-driven biosensor for diamines in *C. glutamicum*. The transcriptional regulator CgmR was shown to be specific for putrescine, cadaverine, 1,6-diaminohexane, and heptanediamine as ligands, especially for longer carbon chain diamines. These findings are different from previous observations of transcription factor PuuR from *E. coli*, which only showed high specificity for putrescine.[14] To improve the performance characteristics of the biosensor, we systematically engineered the genetic components of sensors. Finally, we employed $CgmR_{I152T}$ as well as its cognate promoter and *sfgfp* reporter gene to build the synthetic biosensor $pSenPut_{I152T}$ and then investigate the GFP signal response to both intracellular and extracellular putrescine. The overall strategies described here should be beneficial for the future design and engineering of transcription factor-based biosensors to monitor other valuable cellular metabolites in prokaryotes. The greatest potential for biosensors can be found in genetic variants or pathway evaluations via FACS, which provides a great possibility for characterizing and exploring single cells within the population in cytosolic small molecule concentrations. Consequently, our study demonstrated that the transcription factor CgmR-driven biosensor for diamines in *C. glutamicum* could be an influencing instrument to develop the bioprocess for the production of diamines and polyamide plastics.

MATERIALS AND METHODS

Materials. In this study, all the chemical reagents were obtained from Damao Chemical Reagent Factory (Tianjin, China) or Sigma-Aldrich (St. Louis, MO, USA). Amplification and identification of gene fragments were conducted by KOD DNA polymerase (TOYOBO, Japan) combined with Taq DNA polymerase (Thermo Scientific, Waltham, MA). The NEB Builder HiFi DNA Assembly Master Mix kit (New England BioLabs, Boston, MA) was employed for assembling the plasmids. An Instant Error-prone PCR Kit (Ybio, Shanghai, China) was used to obtain the random mutation library. The constructed plasmids were verified by DNA sequencing (Sangon Biotech, Shanghai, China). Shanghai Generay Biotech Co., Ltd. (Shanghai, China) synthesized all primers and genes.

Bacterial Strains, Plasmids, and Cultivation Media. *E. coli* TOP10, which was applied in the construction of plasmids, was incubated in Luria−Bertani medium (10 g L^{-1} peptone, 5 g L^{-1} yeast extract, and 10 g L^{-1} NaCl) at 37 °C and 200 rpm. *C. glutamicum* ATCC 14067 was incubated in BHI liquid medium (37 g L^{-1} brain heart infusion) (Becton, Dickinson and Co.) or BHISG liquid medium (37 g L^{-1} brain heart infusion, 10 g L^{-1} glucose, and 9.1 g L^{-1} sorbitol) at 30 °C and 220 rpm. The single colony was inoculated in 5 mL of seed medium, which was then cultivated at 220 rpm and 30 °C overnight. The overnight seed incubation sample was inoculated in 50 mL of fermentation medium containing 0.2 initial OD 600. The principal cultures were cultured at 30 °C by using a rotary shaking incubator at 220 rpm. In this study, 80 g glucose, 7.5 g urea, 10 g soya peptone, 0.5 g $MgSO_4$, 0.7 g KH_2PO_4, and 42 g MOPS were included in each liter of fermentation medium. Wherever appropriate, antibiotics were supplemented with concentrations presented as follows: kanamycin at 50 mg L^{-1} (Km), tetracycline at 10 mg L^{-1} (Tet), and chloramphenicol at 20 mg L^{-1} (Cm) for *E. coli* and kanamycin at 25 mg L^{-1} (Km) and tetracycline at 5 mg L^{-1} (Tet) and chloramphenicol at 7.5 mg L^{-1} (Cm) for *C. glutamicum* ATCC 14067. Additionally, isopropyl-*β*-*d*-thiogalactoside (IPTG) concentration, which can be used to generate ornithine decarboxylase expression, reached 0.5 mM. All bacterial strains, plasmids involved in the research, and their corresponding properties are illustrated in Supporting Information Table S1.

Genetic Method. We designed a diamine detection system comprising TR CgmR, a CgmA promoter, as well as the RFP or GFP as the reporter protein. In addition, PCR was used to amplify *cgmR* and *cgmA* promoter fragments based on genomic DNA of *C. glutamicum* ATCC 14067 using the corresponding primers (Supporting Information Table S1). *cgmR* was subcloned downstream in constitutively active promoter P*trc*, while P*cgmA* was inserted onto the contrary side in *cgmR* to avoid transcriptional noises. The synthesized reporter protein genes were subcloned downstream in the *cgmA* promoter. Transcription terminator rrnBT1T2 in plasmid pEC-XK99E was added to *C*-termini in the reporter protein genes as well as *cgmR*. The pSenPut plasmid was built through linking the DNA fragment to plasmid pEC-T18-mob2 for *C. glutamicum*. We also substituted the fluorescent reporter *mCherry* with the *egfp*, *gfp*mut3, and *sfgfp* genes to increase the assay sensitivity. For increasing the pSenPut sensitivity to putrescine, we generated various native promoters of *C. glutamicum* for *cgmR* transcription via PCR and subcloned the two into pSenPut. *cgmR* gene disruption was performed via the RecET-Cre/loxP system as described by Huang et al.[35] The pEC-XK99E plasmid was used for over-expressing all genes associated with putrescine production.

Mutant Library Construction and CgmR Screening. A CgmR mutant library was built through error-prone PCR based on an Instant Error-prone PCR Kit (Ybio, Shanghai, China) with a mutation rate of 0.66% (±0.13%) and using pSenPut as a template. In this study, the fragments, which were employed to build the mutant library, were produced according to standard PCR and linked to the genetic circuit via a NEB Builder HiFi DNA Assembly Master Mix kit (New England BioLabs, Boston, MA). CgmR variants were formed via site-directed mutagenesis using the primer pair 152-S/152-A (Supporting Information Table S1). *E. coli* TOP10 cells experienced transformation via heat shock through recombination mixtures with mutant genes. Plasmid DNA separation and DNA extraction were carried out with the plasmid mini kit purchased from Guangzhou Meiji Biological Co., Ltd. *C. glutamicum* ATCC 14067 Δ*cgmR* was transformed by electroporation through plasmid mixtures with mutant genes. In addition, transformants were distributed on BHISG agar plates with 5 mg L^{-1} tetracycline and subsequently cultivated at 30 °C for 24−36 h. A blue laser (488 nm) was applied in analyzing the fluorescence intensity in the variant library of flow cytometry with a S3e Cell Sorter (Bio-Rad Laboratories, Inc). The associated data analysis was carried out with FlowJo (Tree Star, Ashland, OR, USA). In the first round of screening, the obtained CgmR variants about 1×10^5 transformants were washed and inoculated into 5 mL of BHI medium with 10 mM putrescine and 5 mg L^{-1} tetracycline, followed by incubation at 30 °C for 24 h. The cells were rinsed twice using phosphate-buffered saline (PBS) and subsequently resuspended in the same buffer and diluted to an OD 600 ≈ 0.5 prior to flow

https://doi.org/10.1021/acssynbio.1c00363
ACS Synth. Biol. 2021, 10, 3074−3083

cytometry. Approximately, 2.05 × 10^7 events were analyzed, and the top 0.5% cells with high fluorescence intensity were sorted. In the end, about 10,000 cells were gathered and recovered in BHI medium at 30 °C for 24−36 h. In the second-round screening, false-positive cells exhibiting high fluorescence intensity devoid of putrescine were erased through screening nonfluorescent cells. Around 1.60 × 10^7 events were analyzed, and 0.5% of the bottom nonfluorescent cells in negatively sorted cells was sorted. At last, about 10,000 cells have been gathered and recollected in BHI medium. Until the final round, approximately, 1.54 × 10^7 events were analyzed and the top 0.1% cells with the highest fluorescence in the presence of 10 mM putrescine were sorted. At last, about 800 cells were collected and grown on BHI agar. Finally, 588 variants were isolated by FACS, and 200 variants were analyzed in detail through a 96-well plate. A single clone showing a greater fluorescence intensity compared with cells with wild-type CgmR expression was chosen for performing the in-depth analysis.

CgmR Structure Modeling and Docking Simulations. The homology modeling of the *C. glutamicum* ATCC 14067 CgmR three-dimensional structure was completed using the modeling module of SWISS-MODEL (https://swissmodel.expasy.org/interactive) according to the sequence similarity. The molecular docking and interaction analysis of putrescine was completed using the CDocker molecular docking program in Discovery Studio Client V3.5 software (Accelrys, San Diego, CA, USA), and all docking results were scored and evaluated by the scoring module.

Fluorescence Analysis. For *C. glutamicum* cells harboring pSenPut and pSenPut variants, a fluorescence analysis was performed within the liquid phase. Subsequently, single colonies with pSenPut and pSenPut variants were inoculated in 5 mL of BHI medium with 5 mg L^{-1} tetracycline. After cultivation at 30 °C for 12 h, the cells were diluted at 1:100 into 48- or 96-well plates containing 900 μL or 400 μL of fresh BHI with 5 mg L^{-1} tetracycline, various concentrations of putrescine (0.01−100 mM), and other chemicals (20 mM), for testing ligand specificity. Then, the cells were cultivated at 30 °C and 1000 rpm for 24 h, and the culture broth was rinsed twice using PBS and resuspended in the same buffer for measuring GFP fluorescence in the 96-well plates. For putrescine producers carrying pSenPut, fluorescence analysis of fermentation cultures contained in a shaker flask was performed. The culture broth (100 μL) was collected at the end of fermentation, rinsed twice with PBS, and resuspended in the same buffer for measuring GFP fluorescence, which occurred in 96-well plates. Fluorescence intensity was measured on a multifunctional microplate reader (Infinite M200, Tecan, Switzerland). Optical density was assessed at 600 nm (OD 600), whereas fluorescence was assessed by excitation and emission wavelengths of 584/610 nm for red fluorescent proteins and 488/520 nm for green fluorescent proteins, respectively.

Analytical Methods. The putrescine concentration was decided by the Waters 2695 HPLC system (Waters, USA) containing a SunFire C18 column (100 Å, 5 μm, 4.6 mm × 250 mm). Putrescine was first derivatized using dansyl chloride,[36−38] and the derivatives were detected using a Waters 2489 ultraviolet detector (Waters, USA) at 254 nm. The mobile phase was composed of solvent A (water) and solvent B (acetonitrile). Its flow rate reached 1 mL/min. The gradient used consisted of: 0 min 65% B, 5 min 70% B, 24 min 100% B, and 30 min 65% B. A standard curve was established according to serial dilutions for the standard stock approach for putrescine.

Cell pellets used for intracellular putrescine quantification were rinsed three times in ice-cold water at 13,000 rpm at 4 °C for 5 min. Then, the pellets were resuspended in ice-cold water and lysed with Bead Ruptor 12 (Omni international, Inc., USA). Upon centrifugation, the cell-free lysates were applied to quantify the level of putrescine. The data stands for the mean of three biological replicates, with the error bars corresponding to the standard deviations.

■ ASSOCIATED CONTENT

Supporting Information

The Supporting Information is available free of charge at https://pubs.acs.org/doi/10.1021/acssynbio.1c00363.

Summary of strains, plasmids, and primers used in this study; promoters used in this study for regulating the expression of transcription factor CgmR; biosensor performance parameters; two genetic backgrounds for testing the promoter activity; different versions of pSenPut constructs for optimizing the reporter protein or CgmR expression; response of CgmR to 1,6-diaminohexane (C6) or heptanediamine (C7); FACS-based directed evolution of the CgmR regulator; binding of purified His-tagged CgmR and $CgmR_{I152T}$ to the *cgmO* fragment in the presence of different ligands; and best fitting of biosensor performance parameters and standard deviation (PDF)

■ AUTHOR INFORMATION

Corresponding Authors

Yuanyuan Huang − *Center for Materials Synthetic Biology, Shenzhen Institute of Synthetic Biology, Shenzhen Institutes of Advanced Technology, Chinese Academy of Sciences, Shenzhen 518000, P. R. China*; Email: huangyy@siat.ac.cn

Suiping Zheng − *Guangdong Key Laboratory of Fermentation and Enzyme Engineering, School of Biology and Biological Engineering, South China University of Technology, Guangzhou 510006, P. R. China; Guangdong Research Center of Industrial Enzyme and Green Manufacturing Technology, School of Biology and Biological Engineering, South China University of Technology, Guangzhou 510006, P. R. China*; Email: spzheng@scut.edu.cn

Authors

Nannan Zhao − *Guangdong Key Laboratory of Fermentation and Enzyme Engineering, School of Biology and Biological Engineering, South China University of Technology, Guangzhou 510006, P. R. China; Guangdong Research Center of Industrial Enzyme and Green Manufacturing Technology, School of Biology and Biological Engineering, South China University of Technology, Guangzhou 510006, P. R. China*; orcid.org/0000-0002-2522-1614

Jie Song − *Guangdong Key Laboratory of Fermentation and Enzyme Engineering, School of Biology and Biological Engineering, South China University of Technology, Guangzhou 510006, P. R. China; Guangdong Research Center of Industrial Enzyme and Green Manufacturing Technology, School of Biology and Biological Engineering, South China University of Technology, Guangzhou 510006, P. R. China*

https://doi.org/10.1021/acssynbio.1c00363
ACS Synth. Biol. 2021, 10, 3074−3083

Hao Zhang − *Guangdong Key Laboratory of Fermentation and Enzyme Engineering, School of Biology and Biological Engineering, South China University of Technology, Guangzhou 510006, P. R. China; Guangdong Research Center of Industrial Enzyme and Green Manufacturing Technology, School of Biology and Biological Engineering, South China University of Technology, Guangzhou 510006, P. R. China*

Ying Lin − *Guangdong Key Laboratory of Fermentation and Enzyme Engineering, School of Biology and Biological Engineering, South China University of Technology, Guangzhou 510006, P. R. China; Guangdong Research Center of Industrial Enzyme and Green Manufacturing Technology, School of Biology and Biological Engineering, South China University of Technology, Guangzhou 510006, P. R. China*

Shuangyan Han − *Guangdong Key Laboratory of Fermentation and Enzyme Engineering, School of Biology and Biological Engineering, South China University of Technology, Guangzhou 510006, P. R. China; Guangdong Research Center of Industrial Enzyme and Green Manufacturing Technology, School of Biology and Biological Engineering, South China University of Technology, Guangzhou 510006, P. R. China*

Complete contact information is available at: https://pubs.acs.org/10.1021/acssynbio.1c00363

Author Contributions

N.Z., Y.L., S.H., and S.Z. conceived this project. N.Z. and S.Z. designed the study, explored the data, and completed the manuscript. N.Z. and J.S. carried out the experiments. H.Z. and Y.H. revised the manuscript. All authors read and approved the final manuscript.

Notes

The authors declare no competing financial interest.

■ ACKNOWLEDGMENTS

All the authors are grateful for the financial support of the National Key R&D Program of China (grant no. 2018YFA0901700), the National Natural Science Foundation of China (grant no. 31671840), and the China Postdoctoral Science Foundation (grant no. 2019M661676).

■ REFERENCES

(1) Chae, T. U.; Ahn, J. H.; Ko, Y.-S.; Kim, J. W.; Lee, J. A.; Lee, E. H.; Lee, S. Y. Metabolic engineering for the production of dicarboxylic acids and diamines. *Metab. Eng.* **2020**, *58*, 2−16.

(2) Misawa, N. Pathway engineering for functional isoprenoids. *Curr. Opin. Biotechnol.* **2011**, *22*, 627−633.

(3) Zhao, N.; Qian, L.; Luo, G.; Zheng, S. Synthetic biology approaches to access renewable carbon source utilization in Corynebacterium glutamicum. *Appl. Microbiol. Biotechnol.* **2018**, *102*, 9517−9529.

(4) Binder, S.; Schendzielorz, G.; Stäbler, N.; Krumbach, K.; Hoffmann, K.; Bott, M.; Eggeling, L. A high-throughput approach to identify genomic variants of bacterial metabolite producers at the single-cell level. *Genome Biol.* **2012**, *13*, R40.

(5) Rogers, J. K.; Church, G. M. Genetically encoded sensors enable real-time observation of metabolite production. *Proc. Natl. Acad. Sci. U S A* **2016**, *113*, 2388−2393.

(6) Dietrich, J. A.; McKee, A. E.; Keasling, J. D. High-throughput metabolic engineering: advances in small-molecule screening and selection. *Annu. Rev. Biochem.* **2010**, *79*, 563−590.

(7) Kortmann, M.; Mack, C.; Baumgart, M.; Bott, M. Pyruvate Carboxylase Variants Enabling Improved Lysine Production from Glucose Identified by Biosensor-Based High-Throughput Fluorescence-Activated Cell Sorting Screening. *ACS Synth. Biol.* **2019**, *8*, 274−281.

(8) Chou, H. H.; Keasling, J. D. Programming adaptive control to evolve increased metabolite production. *Nat. Commun.* **2013**, *4*, 2595.

(9) Mahr, R.; Gätgens, C.; Gätgens, J.; Polen, T.; Kalinowski, J.; Frunzke, J. Biosensor-driven adaptive laboratory evolution of l-valine production in Corynebacterium glutamicum. *Metab. Eng.* **2015**, *32*, 184−194.

(10) Grünberger, A.; Wiechert, W.; Kohlheyer, D. Single-cell microfluidics: opportunity for bioprocess development. *Curr. Opin. Biotechnol.* **2014**, *29*, 15−23.

(11) Zhang, J.; Wang, Z.; Su, T.; Sun, H.; Zhu, Y.; Qi, Q.; Wang, Q. Tuning the Binding Affinity of Heme-Responsive Biosensor for Precise and Dynamic Pathway Regulation. *iScience* **2020**, *23*, 101067.

(12) Hicks, M.; Bachmann, T. T.; Wang, B. Synthetic Biology Enables Programmable Cell-Based Biosensors. *Chemphyschem* **2020**, *21*, 132−144.

(13) Ang, J.; Harris, E.; Hussey, B. J.; Kil, R.; McMillen, D. R. Tuning response curves for synthetic biology. *ACS Synth. Biol.* **2013**, *2*, 547−567.

(14) Chen, X.-F.; Xia, X.-X.; Lee, S. Y.; Qian, Z.-G. Engineering tunable biosensors for monitoring putrescine inEscherichia coli. *Biotechnol. Bioeng.* **2018**, *115*, 1014−1027.

(15) Chen, Y.; Ho, J. M. L.; Shis, D. L.; Gupta, C.; Long, J.; Wagner, D. S.; Ott, W.; Josić, K.; Bennett, M. R. Tuning the dynamic range of bacterial promoters regulated by ligand-inducible transcription factors. *Nat. Commun.* **2018**, *9*, 64.

(16) Zhang, F.; Carothers, J. M.; Keasling, J. D. Design of a dynamic sensor-regulator system for production of chemicals and fuels derived from fatty acids. *Nat. Biotechnol.* **2012**, *30*, 354−359.

(17) Thompson, M. G.; Pearson, A. N.; Barajas, J. F.; Cruz-Morales, P.; Sedaghatian, N.; Costello, Z.; Garber, M. E.; Incha, M. R.; Valencia, L. E.; Baidoo, E. E. K.; Martin, H. G.; Mukhopadhyay, A.; Keasling, J. D. Identification, Characterization, and Application of a Highly Sensitive Lactam Biosensor from Pseudomonas putida. *ACS Synth. Biol.* **2020**, *9*, 53−62.

(18) Yeom, S.-J.; Kim, M.; Kwon, K. K.; Fu, Y.; Rha, E.; Park, S.-H.; Lee, H.; Kim, H.; Lee, D.-H.; Kim, D.-M.; Lee, S.-G. A synthetic microbial biosensor for high-throughput screening of lactam biocatalysts. *Nat. Commun.* **2018**, *9*, 5053.

(19) Della Corte, D.; van Beek, H. L.; Syberg, F.; Schallmey, M.; Tobola, F.; Cormann, K. U.; Schlicker, C.; Baumann, P. T.; Krumbach, K.; Sokolowsky, S.; Morris, C. J.; Grünberger, A.; Hofmann, E.; Schröder, G. F.; Marienhagen, J. Engineering and application of a biosensor with focused ligand specificity. *Nat. Commun.* **2020**, *11*, 4851.

(20) Xiong, D.; Lu, S.; Wu, J.; Liang, C.; Wang, W.; Wang, W.; Jin, J.-M.; Tang, S.-Y. Improving key enzyme activity in phenylpropanoid pathway with a designed biosensor. *Metab. Eng.* **2017**, *40*, 115−123.

(21) Tang, S.-Y.; Fazelinia, H.; Cirino, P. C. AraC regulatory protein mutants with altered effector specificity. *J. Am. Chem. Soc.* **2008**, *130*, 5267−5271.

(22) Tang, S.-Y.; Cirino, P. C. Design and application of a mevalonate-responsive regulatory protein. *Angew. Chem., Int. Ed. Engl.* **2011**, *50*, 1084−1086.

(23) Tang, S.-Y.; Qian, S.; Akinterinwa, O.; Frei, C. S.; Gredell, J. A.; Cirino, P. C. Screening for enhanced triacetic acid lactone production by recombinant Escherichia coli expressing a designed triacetic acid lactone reporter. *J. Am. Chem. Soc.* **2013**, *135*, 10099−10103.

(24) Nguyen, A. Q. D.; Schneider, J.; Wendisch, V. F. Elimination of polyamine N-acetylation and regulatory engineering improved putrescine production by Corynebacterium glutamicum. *J. Biotechnol.* **2015**, *201*, 75−85.

(25) Wendisch, V. F.; Mindt, M.; Pérez-García, F. Biotechnological production of mono- and diamines using bacteria: recent progress,

applications, and perspectives. *Appl. Microbiol. Biotechnol.* **2018**, *102*, 3583−3594.
(26) Qian, Z.-G.; Xia, X.-X.; Lee, S. Y. Metabolic engineering of Escherichia coli for the production of putrescine: a four carbon diamine. *Biotechnol. Bioeng.* **2009**, *104*, 651−662.
(27) Kim, H. T.; Baritugo, K.-A.; Oh, Y. H.; Hyun, S. M.; Khang, T. U.; Kang, K. H.; Jung, S. H.; Song, B. K.; Park, K.; Kim, I.-K.; Lee, M. O.; Kam, Y.; Hwang, Y. T.; Park, S. J.; Joo, J. C. Metabolic Engineering of Corynebacterium glutamicum for the High-Level Production of Cadaverine That Can Be Used for the Synthesis of Biopolyamide 510. *ACS Sustainable Chem. Eng.* **2018**, *6*, 5296−5305.
(28) Schneider, J.; Wendisch, V. F. Putrescine production by engineered Corynebacterium glutamicum. *Appl. Microbiol. Biotechnol.* **2010**, *88*, 859−868.
(29) Wang, L.; Li, G.; Deng, Y. Diamine Biosynthesis: Research Progress and Application Prospects. *Appl. Environ. Microbiol.* **2020**, *86*, No. e01972.
(30) Itou, H.; Okada, U.; Suzuki, H.; Yao, M.; Wachi, M.; Watanabe, N.; Tanaka, I. The CGL2612 Protein from Corynebacterium glutamicum Is a Drug Resistance-related Transcriptional Repressor. *J. Biol. Chem.* **2005**, *280*, 38711−38719.
(31) Shang, X.; Chai, X.; Lu, X.; Li, Y.; Zhang, Y.; Wang, G.; Zhang, C.; Liu, S.; Zhang, Y.; Ma, J.; Wen, T. Native promoters of Corynebacterium glutamicum and its application in L-lysine production. *Biotechnol. Lett.* **2018**, *40*, 383−391.
(32) Müller, I. E.; Rubens, J. R.; Jun, T.; Graham, D.; Xavier, R.; Lu, T. K. Gene networks that compensate for crosstalk with crosstalk. *Nat. Commun.* **2019**, *10*, 4028.
(33) Cheng, F.; Tang, X. L.; Kardashliev, T. Transcription Factor-Based Biosensors in High-Throughput Screening: Advances and Applications. *Biotechnol. J.* **2018**, *13*, No. e1700648.
(34) Ding, N.; Yuan, Z.; Zhang, X.; Chen, J.; Zhou, S.; Deng, Y. Programmable cross-ribosome-binding sites to fine-tune the dynamic range of transcription factor-based biosensor. *Nucleic Acids Res.* **2020**, *48*, 10602−10613.
(35) Huang, Y.; Li, L.; Xie, S.; Zhao, N.; Han, S.; Lin, Y.; Zheng, S. Recombineering using RecET in Corynebacterium glutamicum ATCC14067 via a self-excisable cassette. *Sci. Rep.* **2017**, *7*, 7916.
(36) Tasić, T.; Ikonić, P.; Mandić, A.; Jokanović, M.; Tomović, V.; Savatić, S.; Petrović, L. Biogenic amines content in traditional dry fermented sausage Petrovská klobása as possible indicator of good manufacturing practice. *Food Control* **2012**, *23*, 107−112.
(37) Liu, S.-J.; Xu, J.-J.; Ma, C.-L.; Guo, C.-F. A comparative analysis of derivatization strategies for the determination of biogenic amines in sausage and cheese by HPLC. *Food Chem.* **2018**, *266*, 275−283.
(38) Eerola, S.; Hinkkanen, R.; Lindfors, E.; Hirvi, T. Liquid chromatographic determination of biogenic amines in dry sausages. *J. AOAC Int.* **1993**, *76*, 575−577.

https://doi.org/10.1021/acssynbio.1c00363
ACS Synth. Biol. 2021, 10, 3074−3083